Hydrodynamic charge transport in an GaAs/AlGaAs ultrahigh-mobility two-dimensional electron gas

Xinghao Wang, Peizhe Jia, Rui-Rui Du, L. N. Pfeiffer, K. W. Baldwin, and K. W. West

Phys. Rev. B **106**, L241302 — Published 22 December 2022

DOI: 10.1103/PhysRevB.106.L241302

Hydrodynamic charge transport in GaAs/AlGaAs ultrahigh-mobility two-dimensional electron gas

Xinghao Wang*, Peizhe Jia, and Rui-Rui Du**

International Center for Quantum Materials, School of Physics, Peking University, Beijing 100871, China

L. N. Pfeiffer, K. W. Baldwin, and K. W. West

Department of Electrical Engineering, Princeton University, Princeton, NJ 08544, USA

Abstract

Viscous fluid in an ultrahigh-mobility two-dimensional electron gas (2DEG) in GaAs/AlGaAs quantum wells is systematically studied through measurements of negative magnetoresistance (NMR) and photoresistance under microwave radiation, and the data are analyzed according to recent theoretical work by *e.g.*, Alekseev, Physical Review Letters **117**,166601 (2016). Size-dependent and temperature dependent NMR are found to conform to the theoretical predictions. The size dependence of microwave induced resistance oscillations and that of the '2nd harmonic' peak indicate that 2DEG in a moderate magnetic field should be regarded as viscous fluid as well. Size-dependent radiation heating effect is found by using NMR as electron thermometry. Our results suggest that the hydrodynamic effects must be considered in order to understand semiclassical electronic transport in a clean 2DEG.

* 17wxhwypku@pku.edu.cn
** rrd@pku.edu.cn

Introduction. - Hydrodynamic charge transport in high-mobility 2D electron systems has been discussed theoretically for decades [1–8], but it does not arouse great attention until recently, as evidence of viscous liquid has been discovered in 2D metal $PdCoO_2$ [9], graphene [10, 11] and GaAs/AlGaAs quantum well (QW) [12-17]. As the cleanest electron system available so far, GaAs/AlGaAs QW is a natural material manifesting rich hydrodynamic properties through NMR [18–26], exotic photoresistance (PR) induced by microwave radiation [18, 20, 21], nonlocal resistance measurement [13, 17], Hall viscosity [14] and other method such as geometric control[16] and scanning gate microscopy[15]. However, NMR and PR, as the focusing point of this paper, were not understood with respect to viscosity of electron fluid in the early prints, rather, *e.g.*, as that of an interplay between smooth long-range disorder and rare strong scatterers [27], until theories of viscous flow in moderate magnetic field (when Landau levels are not well resolved) in 2DEG were proposed by *e.g.*, Alekseev, and others [28–33].

For 2DEG with sample width W, hydrodynamic regime is defined to be $l_{ee} \ll W^2/l_{ee} \ll l_0$. Respectively, l_{ee}, l_0 is the mean free path (MFP) for momentum conserving collisions between quasiparticles (electrons), and momentum relaxing bulk collisions between electrons and impurities or phonons. Under this condition, sheer stress among electrons may result in hydrodynamic transport with many intriguing effects to be explored. Together with ballistic transport, viscosity of electron fluid gives rise to a charged Poiseuille flow with enhanced zero-field resistivity $\rho_{xx}(0) \propto W^{-2}$ and temperature-dependent NMR [28]. Moreover, giant PR peak at microwave (MW) frequency $\omega = 2\omega_c$ ('2nd harmonic' for short) observed in [18, 20], where $\omega_c = eB/m^*$ is cyclotron frequency, can be explained qualitatively by the theory of transverse magnetosonic waves caused by shear stress in Fermi liquid [30]. More recently, hydrodynamics in 2DEG has been applied to microwave-induced resistance oscillations (MIRO) [34–36], and significant predictions were proposed in [33]. The present experiments, specifically using ultrahigh-mobility GaAs/AlGaAs QW samples, are partly promoted by these theoretical works.

In this letter, hydrodynamics of 2DEG in modulation-doped GaAs/AlGaAs QW is systematically studied in low temperature transport experiments performed in a ^{3}He refrigerator with three ultrahigh-mobility wafers (with a nominal mobility μ above $2 * 10^7 cm^2/Vs$ at 0.3 K), carrier density n of which ranges from $2.0 * 10^{11}\ cm^{-2}$ to $4.2 * 10^{11}\ cm^{-2}$. Each sample consists of five sections of Hall bars with different sample widths ($W = 400, 200, 100, 50, 25\ \mu m$) and the same length-to-width ratio $L/W = 3$, defined by photolithography and wet etching. Electrical contacts were made by In/Sn alloy. For details of each sample and structure of Hall bars, please refer to Table SI [46] and inset of Fig.1(a).

Our experiments found some intriguing hydrodynamic effects of the 2D electron fluid. NMR induced by both viscoelastic effect and ballistic transport is perfectly consistent with theoretical work [28, 32]. For instance, zero-field resistivity linear with $1/W^2$ was verified at the first time, and temperature dependence of the NMR conformed to some theoretical work so well that crossover of viscous gas and viscous liquid could be distinguished. As for PR, '2nd harmonic' peaks observed in all our samples reaffirmed the hydrodynamic effect in moderate magnetic field. Additionally, W-dependence of the MIRO amplitude conforms to the predictions by [33], which might pose a challenge to the non-hydrodynamic theories proposed to explain MIRO. Size-dependent radiation heating effect further demonstrates how hydrodynamics influences MIRO. Altogether, the experimental results affirmatively and consistently support the viscous liquid theory of 2DEG [28–33].

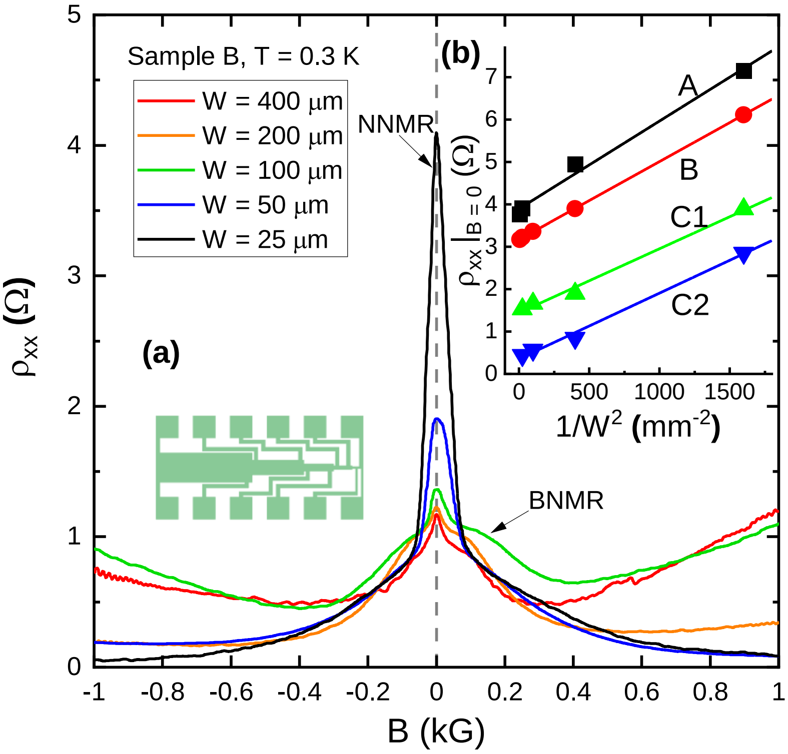

FIG. 1. NMR of Sample B as an example with Hall bar width ranges from 400 μm to 25 μm at 0.3 K. BNMR and NNMR can be distinguished in all five traces. Inset (a) shows configuration of the Hall bar in our experiment. Inset (b) demonstrates linear relation between zero-field resistivity and $1/W^2$ in all the four samples. For clarity, respective data for sample A, B, C1, C2 is consecutively shifted upward by 1 Ω.

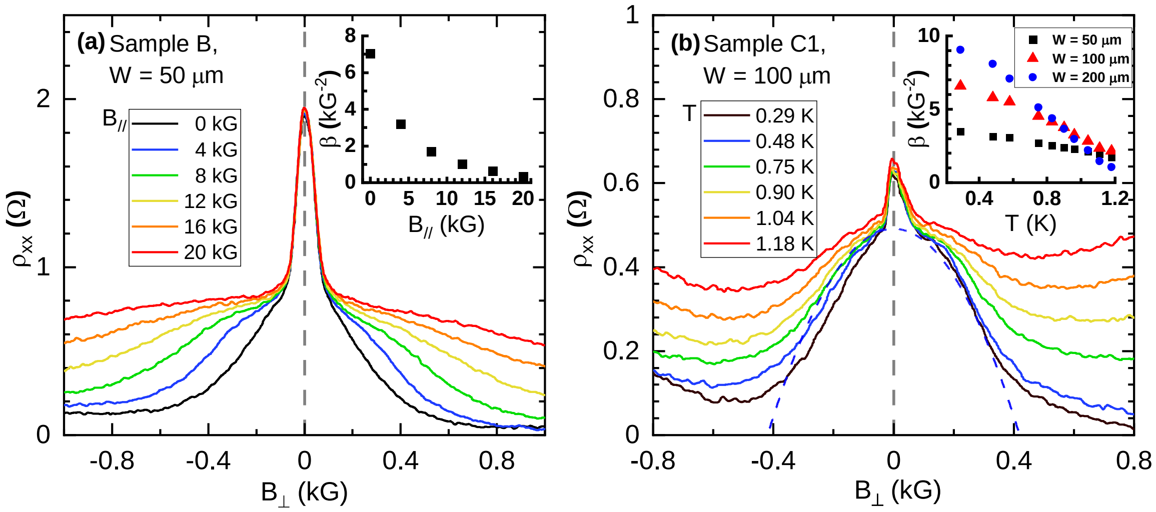

FIG. 2. (a) NNMR is not affected by in-plane magnetic field, but BNMR is. The data is measured from 50 μm Hall bar of Sample B at 0.3 K. The inset shows the relation between β from Eq. (4) and the in-plane field. (b) Higher temperature suppresses BNMR more quickly than NNMR. The data is measured from $100\ \mu m$ Hall bar of Sample C1. The blue dashed curve is fit to the data at 0.48 K as an example. The inset demonstrates temperature dependence of β with three different widths in Sample C1.

Negative magnetoresistance. -As an example, Fig.1 demonstrates the key feature of NMR for different sample widths. The NMR consists of two distinct parts: a narrow, sensitively sample-size-dependent peak (NNMR) dominating within ±100 G and a broad 'bell-shaped' NMR (BNMR) whose maximum resistivity hardly depends on W. These two coexisting parts were also reported in previous experiments[18–24, 26] and can be discriminated from each other, for BNMR is easily suppressed by adding a moderate in-plane magnetic field ($B_{\parallel} < 10\ kG$) or warming up to several kelvins[22], as clearly shown in Fig. 2(a) and (b). However, these early reports suggested that NNMR is caused by weak localization or oval defects in GaAs/AlGaAs QWs. In hindsight, this was partly because their samples were too wide to form a distinguished NNMR.

Recently, NMR in a high density 2DEG of GaAs/AlGaAs QW has been reported and explained within the framework of hydrodynamics[12-14], but BNMR was not observed there. This led to a question whether NNMR and BNMR are both related to viscosity. A theoretical work[37] suggested that NNMR is probably the result of ballistic transport and BNMR is caused by viscosity. Our experiments, however, partly contradicted with their analysis, proving that NNMR is caused by viscoelastic dynamics together with ballistic transport of 2D electron fluid and BNMR seems do not originate from any known hydrodynamic effect.

From theoretical perspectives, Poiseuille flow of electrons results in an effective relaxation time $\tau^* = W^2/12\eta$, where $\eta = (v_F^\eta)^2\tau_2/4$ represents viscosity of electron fluid[28]. v_F^η is the Fermi velocity corrected by viscosity η[30]. τ_2 is the relaxation time of the second moment of the electron distribution function, including contributions from quasiparticle-quasiparticle (electron-electron) collision part $\tau_{2,ee}$ and temperature-independent part $\tau_{2,0}$ determined by electrons scattered on sample edge, which is related to ballistic transport. τ_2 satisfies reciprocal rule $1/\tau_2 = 1/\tau_{2,ee} + 1/\tau_{2,0}$. With a finite magnetic field, viscosity is attenuated due to loss of shear stress and magnetoresistivity is represented approximately as [28]

$$\rho_{xx}(B) = \frac{m^*}{e^2 n}\left(\frac{1}{\tau_0} + \frac{1}{\tau^*(1+(2\omega_c\tau_2)^2)}\right), \quad (1)$$

where $m^* = 0.067m_e$ for GaAs and m_e is the mass of free electron. Inset (b) of Fig.1 shows that zero-field resistivity $\rho_{xx}(0)$ is linear with $1/W^2$ in all the four samples, which is in correspondence with Eq.(1). This result indicates that NNMR matches the viscosity-related NMR described in [28]. v_F^η fitted in this method is smaller than Fermi velocity (Table. SI). This can be remedied if we consider that when boundary scattering becomes important in narrow samples, further correction $\tau^* = W(W + 6l_s)/12\eta$ is more appropriate, where l_s is boundary slip length[26]. A recent work acquiring a controllable boundary slip condition confirmed this conjecture [16].

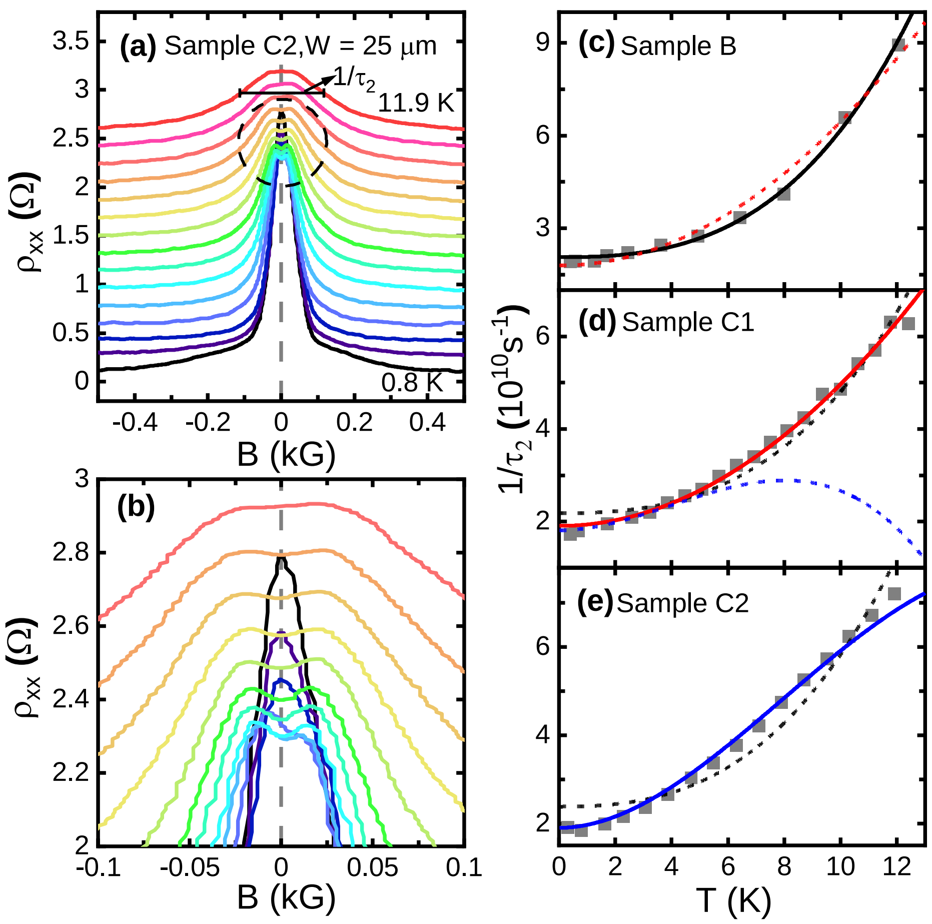

FIG. 3. (a) Magnetoresistivity of Sample C2 at different temperatures from 0.8 K to 11.9 K, with $1/\tau_2$ extracted from the full width half maximum of NNMR. (b) Zoom in of Fig. 3 (a) shows details of NNMR near zero field. Gray squares in (c)(d)(e) are the extracted data from 25 μm Hall bars of Sample B, C1 and C2 respectively. The data is fitted assuming $1/\tau_2(T) = 1/\tau_{2,ee}(T) + 1/\tau_{2,0}$, with three different functions of $1/\tau_{2,ee}$: Eq. (2) in black, Eq. (3) in blue, and $1/\tau_{2,ee} \propto T^2$ in red. (c) For Sample B with $r_s = 1.09$, Eq. (2) fits quite well. (d) For Sample C1 with $r_s = 0.92$, $1/\tau_{2,ee}$ is proportional to T^2. (e) For Sample C2 with $r_s = 0.86$, Eq. (3) fits well below 10 K. Difference among these samples shows density related crossover between viscous fluid and viscous gas.

At higher temperature ($T > 4K$), NNMR is dominated by hydrodynamic charge transport, which is proved in Fig. 3 showing temperature dependence of $1/\tau_2$ in wafer B and C. Paper [32] suggested that electron systems in the two hydrodynamic regimes (liquid or gas) should crossover depending on the strength of Coulomb interactions. For low density 2DEG, interparticle interaction parameter $r_s = 1/(\sqrt{\pi n} a_B)$ is on the order of 1 ($a_B = 10\ nm$, is Bohr radius in GaAs), and electron-electron scattering relaxation time [7]

$$\frac{1}{\tau_{2,ee}} \propto \frac{T^2}{\ln^2(\epsilon_F/k_B T)}, \quad (2)$$

where T is electron temperature, k_B refers to Boltzmann constant, and ϵ_F is Fermi energy of 2DEG. This regime is called viscous liquid for the strong interaction between particles. However, for high density 2DEG with $r_s \ll 1$, which is described as viscous gas, $\tau_{2,ee}$ can be expressed with a different logarithmic factor [32]:

$$\frac{1}{\tau_{2,ee}} = \frac{8\pi}{3\hbar} \frac{(k_B T)^2 r_s^2}{\epsilon_F} \ln\left(\frac{1}{r_s + T/\epsilon_F}\right), \quad (3)$$

where $\hbar$ represents Planck constant divided by 2π. Despite the fact that density of ordinary ultrahigh-quality 2DEG in GaAs QW lies in the regime of viscous liquid and thus $\tau_{2,ee}$ should obey Eq. (2), viscous-gas-like temperature dependence of τ_2 of Sample C1 with $r_s = 0.92$ and C2 with $r_s = 0.86$ seems to indicate electrons in it are within a crossover phase between the viscous liquid and gas described by Eq. (2) and (3). In Fig.3(c), Sample B possesses a stronger Coulomb interaction ($r_s = 1.09$) and its $\tau_{2,ee}$ is fitted quite well with Eq. (2), confirming the hydrodynamic nature of NNMR. For wafer C (Fig. 3(d) and (e)), $\tau_{2,ee}$ is fitted precisely with Eq. (3) as long as $1 - r_s \gg T/\epsilon_F$ (so that temperature dependence in logarithmic factor of Eq. (3) can be ignored) but much off with Eq. (2). This means at low temperatures Eq. (3) accurately describes the interparticle relaxation time in wafer C. This result clearly confirms the viscoelastic dynamics theory in [32] but, a caveat should be noted here. Despite its viscous gas like temperature dependence of τ_2, Sample C1 and C2 cannot be classified into viscous gas because strong '2nd harmonic' peaks are discovered in them (to be presented in Fig.4(b)), which is a typical feature of viscous liquid. Our results present an interesting case for further studies into the crossover region where existing theory does not fully address.

As for BNMR, its shape (Fig. 1) is a parabolic curve[22]:

$$\rho_{xx}(B) = \rho_{xx}(0)(1 - \beta B^2), \tag{4}$$

attributed to a field-independent correction to longitudinal magnetoconductance $\Delta\sigma_{xx}$ in previous work [40]. Here $\rho_{xx}(0)$ does not contain contribution from NNMR and, according to our analysis, only depends on momentum relaxing scatterings. Similar 'bell-shaped' NMR [41, 42] in lower mobility samples was explained through interaction correction theories [27, 40, 43] and $\Delta\sigma_{xx}$ was proved to be proportional to $-\ln(T)$ or $1/\sqrt{T}$ in different regimes. However, in recent reports [22-24], the existing theory is unable to explain BNMR in high purity samples for its peculiar relation between β and T, and, more importantly, the influence of in-plane magnetic field (Fig. 2(a)). We confirm that BNMR is a size-dependent effect since β is approximately proportional to sample width W (Inset of Fig. 2(b)) and this explains why BNMR was not observed in narrow samples ($W \sim 5\mu m$) [12]. BNMR is hardly the result of viscosity because (i) its $\rho_{xx}(0)$ is almost independent of W and (ii) relation between β and W qualitatively contradicts with the characteristics of Poiseuille flow, i.e., Eq. (1).

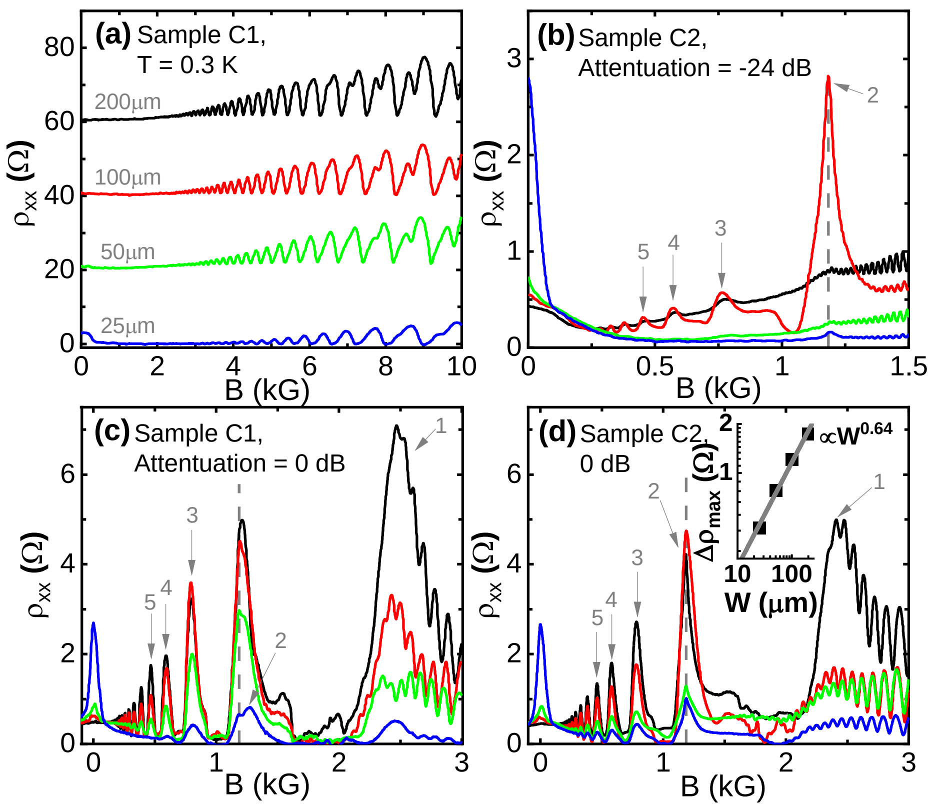

FIG. 4. (a) SdH oscillations of Sample C1 without MW at 0.3 K. For clarity, each ρ_{xx} trace except that of 25 μm is consecutively shifted upwards by 20 Ω. (b)(c)(d) Traces of PR at 0.3 K with different colors are taken from Hall bars with different widths: $200\ \mu m$ (black), $100\ \mu m$ (red), $50\ \mu m$ (green), $25\ \mu m$ (blue). Gray dashed line indicates the '2nd harmonic' peak at exactly $\omega = 2\omega_c$ and first five MIRO peaks are marked with gray arrows. (b) MIRO of Sample C2 with attenuation equal to -24 dB shows a sharp '2nd harmonic' peak for $100\ \mu m$ Hall bar. (c) and (d): MIRO of Sample C1 and C2 without MW attenuation. The inset of (d) shows the relation of MIRO amplitude and sample width when $\omega > 2\omega_c$. The amplitude is fitted with the field-dependent term removed, following the method of paper[44].

Microwave-induced resistance oscillations and 'second harmonics'. - Providing further evidence for the hydrodynamic theory, this section focuses on W-dependence of MIRO. In our experiment, MW with a frequency of 102.4 GHz was produced by a Gunn oscillator, whose power was attenuated by a programmable rotary vane attenuator.

Fig. 4(c) and (d) demonstrate the W-dependence of the PR. For Hall bar with different W, Shubonikov-de Hass (SdH) oscillation is shown in Fig. 4(a) with almost invariant quantum scattering time and oscillation magnitude. Compared with SdH oscillation, MIRO of all samples markedly depends on W in an opposite way of NNMR. In a Poiseuille flow, sample width determines the maximum of electron velocity, and therefore, there's a positive correlation between zero-field conductance/photoconductance and W. However, zero-field resistance is reciprocal of conductance, while PR is proportional to photoconductance because of large Hall resistance, giving rise to opposite W-dependence between NNMR and MIRO.

The amplitude of PR peak near $\omega = \omega_c$, *i.e.*, the first peak, is approximately linear with W, strongly favoring the theoretical prediction [33]. The amplitude $\Delta\rho_{max}$ in lower field ($\omega > 2\omega_c$) is found to be proportional to $W^{0.64}$ (Inset of Fig. 4 (d)), which approximately follows the linear dependence of W for wide samples, *i.e.*, $W \gg v_F^{\eta}\tau_2$. W-dependence of the PR contradicts with most of the existing theories explaining MIRO, except the hydrodynamic theory.

As a concomitant phenomenon, the '2nd harmonic' peak could be viewed as evidence for the hydrodynamic theory of MIRO. As examples shown in Fig. 4, '2nd harmonic' peak located precisely at $\omega = 2\omega_c$ is observed in all the four samples, more clearly in relatively narrow Hall bars. In particular, strong '2nd harmonic' is observed in $100\mu m$ Hall bar of wafer C2 (Fig. 4(b)). There's always a tiny peak at $\omega = 2\omega_c$ when MIRO almost disappears in Fig. 4(b). This is due to the fact that the amplitude of MIRO declines faster when MW power is weakened. According to the viscosity theory [30, 33], we can understand the competition between MIRO and the '2nd harmonic' when W is varied. On one hand, transverse magnetosonic waves, origin of '2nd harmonic', prevail only when viscoelastic resonance overweighs magnetoplasmon effect. So relevant upper limit for W is the characteristic wavelength of magnetoplasmons. On the other hand, the dc PR peak originating from ac viscoelastic resonance at $\omega = 2\omega_c$ is size-dependent just like MIRO, *i.e.*, narrower sample corresponds to weaker PR. On balance there exists an optimal sample size for '2nd harmonic' peak and the value appears to be around $100\ \mu m$ for Sample C. Our data strongly support the viscoelastic nature of both MIRO and the 'second harmonic' for ultrahigh-mobility 2DEG under microwave radiation.

Size-dependent radiation heating effect. -The sensitive temperature-dependence of BNMR can be used as a natural electron thermometry in the temperature range of $0.3\ K$ to $2\ K$. With MW irradiated onto 2DEG, electrons are warmed up to a temperature T_e higher than that of the surroundings $T_s = 0.3\ K$, inducing a MW-dependent BNMR before MIRO takes place. This effect is due to relatively low thermoconductance between 2DEG and surroundings.

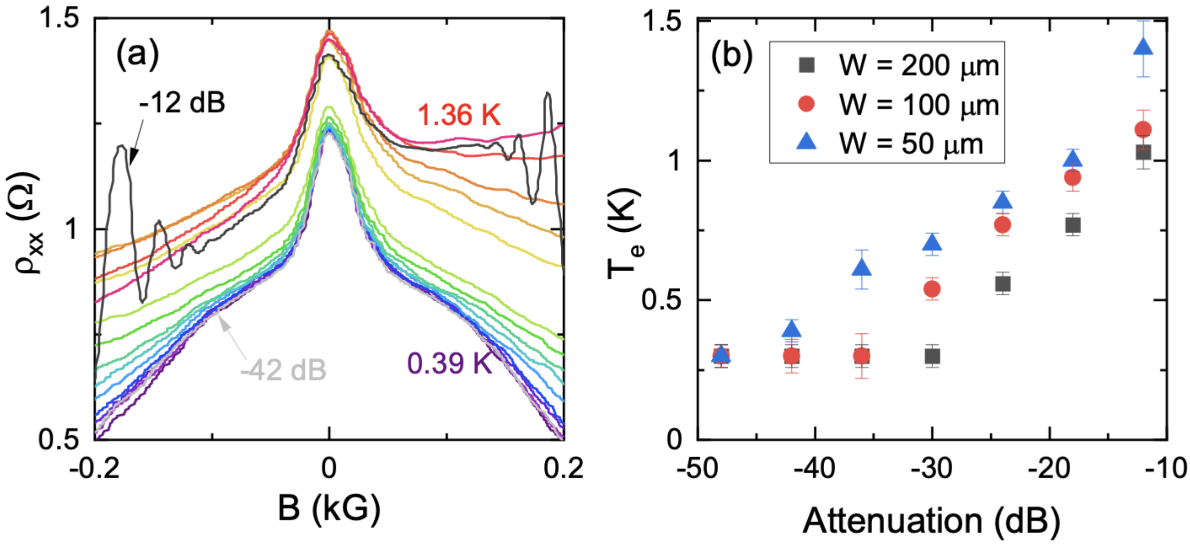

FIG. 5. (a) Temperature dependence of BNMR can be used to calibrate T_e. MIRO with MW attenuation equal to -12 dB (-42 dB) is shown in the black (gray) line. MW frequency is about 30 GHz and the data is obtained from the $100\ \mu m$ section of another sample of Wafer B. (b) T_e in Hall bar with $W = 200\ \mu m, 100\ \mu m, 50\ \mu m$ shows that electrons in narrower section are hotter than those in wider section.

An example of the heating effect is demonstrated in Fig.5(a). Despite T_s remaining 0.3K, however, the MIRO trace is lifted up when MW power is enhanced. Compared with BNMR traces without MW, the MIRO trace shows its T_e. T_e of the $W = 100\ \mu m$ section is above 1K with MW attenuation equal to -12 dB, while remains almost the same as T_s when attenuation is -42 dB.

In Fig.5(b), temperature-dependence of MW power in three different sections is demonstrated, which unambiguously indicates that narrower section of Hall bar features higher T_e. This effect, suggesting that narrower section of 2DEG absorbs more amount of MW, is found in all the samples and could be understood together with Drude model and hydrodynamic theory. The absorbed power of MW is $\Delta P_a =< Re(\hat{E}^* \sigma \hat{E}) >$, where ac conductivity of 2DEG is $\sigma^{\pm} = en\mu/(1 - i(\omega \pm \omega_c\ )\tau)$ and $\pm$ represents circularly left/right polarized radiation. The absorption rate $\Delta P_a/P_i$ is [45]

$$\frac{\Delta P_a}{P_i} = \Sigma_{\pm} \frac{Re(\sigma^{\pm} Z_0)}{[1 + \kappa + Re(\sigma^{\pm} Z_0)]^2 + [Im(\sigma^{\pm} Z_0)]^2},$$

where the refractive index κ is 3.6 for GaAs and $Z_0 = \sqrt{\mu_0/\epsilon_0}$ is the impedance of free space. For narrower width W, hydrodynamic flow of electrons gives rise to a smaller mobility μ, thus resulting in a higher MW absorption rate. This indicates that the size-dependent radiation heating effect is also in accord with hydrodynamic nature of the 2DEG. With more MW absorption, narrower section of 2DEG still features much weaker MIRO. In this way, the smaller exponent 0.64 of size-dependent MIRO $\Delta\rho_{max}$ is partly explained.

Conclusion. -Width-dependence and temperature-dependence of NMR in ultrahigh-mobility 2DEG is in accordance with recent viscoelastic dynamics theory. Furthermore, existence of '2nd harmonic' peak and width-dependence of MIRO also indicates that 2DEG in semi-classical regime (B < a few kG) should be taken as viscous fluid. Overall, the intriguing experimental findings reported here strongly support viscous fluid theory of electrons in ultrahigh-mobility GaAs/AlGaAs QWs, not only in the regime of weak magnetic field but also in moderate magnetic field. It is interesting to note that, as the GaAs/AlGaAs QWs have reached the ultrahigh-mobility regime, it becomes necessary to consider the hydrodynamic effect in assessing the quality of the 2DEG, in addition to the Drude mobility from impurity scatterings.

Acknowledgements. The work at PKU was funded by the National Key R&D Program of China (Grants No. 2017YFA0303300 and 2019YFA0308400), by the Strategic Priority Research Program of Chinese Academy of Sciences (Grant No. XDB28000000). The work at Princeton was funded by the Gordon and Betty Moore Foundation through the EPiQS initiative Grant No. GBMF4420, by the National Science Foundation MRSEC Grant No. DMR-1420541.

References

[1] R. N. Gurzhi, A. N. Kalinenko, and A. I. Kopeliovich, "Electron-electron collisions and a new hydrodynamic effect in two-dimensional electron gas", Phys. Rev. Lett. 74, 3872 (1995).

[2] H. Buhmann, L. W. Molenkamp, R. N. Gurzhi, A. N. Kalinenko, A. I. Kopeliovich, and A. V. Yanovsky, "On dynamic properties of a two-dimensional degenerate electron gas", Low Temp. Phys. **24**, 737 (1998).

[3] H. Predel, H. Buhmann, L. W. Molenkamp, R. N. Gurzhi, A. N. Kalinenko, A. I. Kopeliovich, and A. V. Yanovsky, "Effects of electron-electron scattering on electron-beam propagation in a two-dimensional electron gas", Phys. Rev. B **62**, 2057 (2000).

[4] M. Hruska and B. Spivak, "Conductivity of the classical two-dimensional electron gas", Phys. Rev. B **65**, 033315 (2002).

[5] A. V. Andreev, S. A. Kivelson, and B. Spivak, "Hydrodynamic description of transport in strongly correlated electron systems", Phys. Rev. Lett. **106**, 256804 (2011).

[6] A. Tomadin, G. Vignale, and M. Polini, "Corbino disk viscometer for 2D quantum electron liquids", Phys. Rev. Lett. **113**, 235901 (2014).

[7] D. S. Novikov, "Viscosity of a two-dimensional Fermi liquid", arXiv preprint cond-mat/0603184v1.

[8] M. Mendoza, H. J. Herrmann, and S. Succi, "Hydrodynamic model for conductivity in graphene", Sci. Rep. **3**, 1052 (2013).

[9] P. J. W. Moll, P. Kushwaha, N. Nandi, B. Schmidt, and A. P. Mackenzie, "Evidence for hydrodynamic electron flow in PdCoO□", Science **351**, 1061 (2016).

[10] D. A. Bandurin, I. Torre, R. K. Kumar, M. B. Shalom, A. Tomadin, A. Principi, G. H. Auton, E. Khestanova, K. S. Novoselov, I. V. Grigorieva, et al., "Negative local resistance caused by viscous electron backflow in graphene", Science **351**, 1055 (2016).

[11] R. K. Kumar, D. A. Bandurin, F. M. D. Pellegrino, Y. Cao, A. Principi, H. Guo, G. H. Auton, M. B. Shalom, L. A. Ponomarenko, G. Falkovich, et al., "Superballistic flow of viscous electron fluid through graphene constrictions", Nat. Phys. **13**, 1182 (2017).

[12] G. M. Gusev, A. D. Levin, E. V. Levinson, and A. K. Bakarov, "Viscous electron flow in mesoscopic two-dimensional electron gas", AIP Adv. **8**, 025318 (2018).

[13] A. D. Levin, G. M. Gusev, E. V. Levinson, Z. D. Kvon, and A. K. Bakarov, "Vorticity-induced negative nonlocal resistance in a viscous two-dimensional electron system", Phys. Rev. B **97**, 245308 (2018).

[14] G. M. Gusev, A. D. Levin, E. V. Levinson, and A. K. Bakarov, “Viscous transport and Hall viscosity in a two-dimensional electron system”, Phys. Rev. B **98**, 161303(R) (2018).

[15] B. A. Braem, et.al., “Scanning gate microscopy in a viscous electron fluid”, Phys. Rev. B 98, 241304(R) (2018).

[16] A. C. Keser, et al., “Geometric control of universal hydrodynamic flow in a two-dimensional electron fluid”, Phys. Rev. X 11, 031030 (2021).

[17] A. Gupta, J. J. Heremans, G. Kataria, M. Chandra, S. Fallahi, G. C. Gardner and M. J. Manfra, “Hydrodynamic and ballistic transport over large length scales in GaAs/AlGaAs”, Phys. Rev. Lett. 126, 076803 (2021).

[18] Y. Dai, R. R. Du, L. N. Pfeiffer, and K. W. West, “Observation of a cyclotron harmonic spike in microwave-induced resistances in ultraclean GaAs/AlGaAs quantum wells”, Phys. Rev. Lett. **105**, 246802 (2010).

[19] L. Bockhorn, P. Barthold, D. Schuh, W. Wegscheider, and R. J. Haug, “Magnetoresistance in a high-mobility two-dimensional electron gas”, Phys. Rev. B **83**, 113301 (2011).

[20] A. T. Hatke, M. A. Zudov, L. N. Pfeiffer, and K. W. West, **“**Giant microwave photoresistivity in high-mobility quantum Hall systems**”,** Phys. Rev. B 83, 121301(R) (2011).

[21] Y. Dai, K. Stone, I. Knez, C. Zhang, R. R. Du, C. Yang, L. N. Pfeiffer, and K. W. West, “Response of the microwave-induced cyclotron harmonic resistance spike to an in-plane magnetic field”, Phys. Rev. B **84**, 241303(R) (2011).

[22] A. T. Hatke, M. A. Zudov, J. L. Reno, L. N. Pfeiffer, and K. W. West, “Giant negative magnetoresistance in high-mobility two-dimensional electron systems”, Phys. Rev. B **85**, 081304(R) (2012).

[23] R. G. Mani, A. Kriisa, and W. Wegscheider, “Size-dependent giant-magnetoresistance in millimeter scale GaAs/AlGaAs 2D electron devices”, Sci. Rep. **3**, 2747 (2013).

[24] L. Bockhorn, A. Hodaei, D. Schuh, W. Wegscheider, and R. J. Haug, “Magnetoresistance in a high mobility two-dimensional electron system as a function of sample geometry”, J. Phys.: Conf. Ser. **456**, 012003 (2013).

[25] Q. Shi, P. D. Martin, Q. A. Ebner, M. A. Zudov, L. N. Pfeiffer, and K. W. West, “Colossal negative magnetoresistance in a two-dimensional electron gas”, Phys. Rev. B **89**, 201301(R) (2014).

[26] L. Bockhorn, I. V. Gornyi, D. Schuh, C. Reichl, W. Wegscheider, and R. J. Haug, “Magnetoresistance induced by rare strong scatterers in a high-mobility two-dimensional electron gas”, Phys. Rev. B **90**, 165434 (2014).

[27] A. D. Mirlin, D. G. Polyakov, F. Evers, and P. Wölfle, “Quasiclassical negative magnetoresistance of a 2D electron gas: interplay of strong scatterers and smooth disorder”, Phys. Rev. Lett. **87**, 126805 (2001).

[28] P. S. Alekseev, “Negative magnetoresistance in viscous flow of two-dimensional electrons”, Phys. Rev. Lett. **117**, 166601 (2016).

[29] P. S. Alekseev, “Magnetic resonance in a high-frequency flow of a two-dimensional viscous electron fluid”, Phys. Rev. B **98**, 165440 (2018).

[30] P. S. Alekseev and A. P. Alekseeva, “Transverse magnetosonic waves and viscoelastic resonance in a two-dimensional highly viscous electron fluid”, Phys. Rev. Lett. **123**, 236801 (2019).

[31] P. S. Alekseev, “Magnetosonic waves in a two-dimensional electron Fermi liquid”, Semiconductors **53**, 1367 (2019).

[32] P. S. Alekseev and A. P. Dmitriev, “Viscosity of two-dimensional electrons”, Phys. Rev. B **102**, 241409(R) (2020).

[33] P. S. Alekseev and A. P. Alekseeva, “Microwave-induced resistance oscillations in highly viscous electron fluid”, arXiv preprint arXiv:2105.01035v2.

[34] M. A. Zudov, R. R. Du, J. A. Simmons, and J. L. Reno, “Shubnikov–de Haas-like oscillations in millimeterwave photoconductivity in a high-mobility two-dimensional electron gas”, Phys. Rev. B **64**, 201311(R) (2001).

[35] P. D. Ye, L. W. Engel, D. C. Tsui, J. A. Simmons, J. R. Wendt, G. A. Vawter, and J. L. Reno, “Giant microwave photoresistance of two-dimensional electron gas”, Appl. Phys. Lett. **79**, 2193 (2001).

[36] R. G. Mani, J. H. Smet, K. von Klitzing, V. Narayanamurti, W. B. Johnson, and V. Umansky, “Zero-resistance states induced by electromagnetic-wave excitation in GaAs/AlGaAs heterostructures”, Nature **420**, 646 (2002).

[37] A. N. Afanasiev, P. S. Alekseev , A. A. Greshnov, and M. A. Semina, “Ballistic-hydrodynamic phase transition in flow of two-dimensional electrons”, Phys. Rev. B **104**, 195415 (2021).

[38] I. Mandal and A. Lucas, “Sign of viscous magnetoresistance in electron fluids”, Phys. Rev. B **101**, 045122 (2020).

[39] Y. Huang and M. Wang, “Nonnegative magnetoresistance in hydrodynamic regime of electron fluid transport in two-dimensional materials”, Phys. Rev. B **104**, 155408 (2021).

[40] A. Houghton, J. R. Senna, and S. C. Ying, “Magnetoresistance and Hall effect of a disordered interacting two-dimensional electron gas”, Phys. Rev. B, **25**, 2196 (1982).

[41] M. A. Paalanen, D. C. Tsui, and J. C. M. Hwang, “Parabolic magnetoresistance from the interaction effect in a two-dimensional electron gas”, Phys. Rev. Lett. **51**, 2226 (1983).

[42] L. Li, Y. Y. Proskuryakov, A. K. Savchenko, E. H. Linfield, and D. A. Ritchie, “Magnetoresistance of a 2D electron gas caused by electron interactions in the transition from the diffusive to the ballistic regime”, Phys. Rev. Lett. **90**, 076802 (2003).

[43] S. M. Girvin, M. Jonson, and P. A. Lee, “Interaction effects in disordered Landau-level systems in two dimensions”, Phys. Rev. B **26**, 1651 (1982).

[44] A. T. Hatke, M. A. Zudov, L. N. Pfeiffer, and K. W. West, “Temperature dependence of microwave photoresistance in 2D electron systems”, Phys. Rev. Lett. **102**, 066804 (2009).

[45] S. A. Studenikin, M. Potemski, A. Sachrajda, M. Hilke, L. N. Pfeiffer, and K. W. West, “Microwave-induced resistance oscillations on a high-mobility two-dimensional electron gas: Exact waveform, absorption/reflection and temperature damping”, Phys. Rev. B **71**, 245313 (2005).

[46] Supplemental materials.